FILAMENTATION OF VOLCANIC PLUMES ON THE JOVIAN SATELLITE IO

ANTHONY L. PERATT

Los Alamos National Laboratory, Los Alamos, New Mexico, U.S.A.

and

A. J. DESSLER

Department of Space Physics and Astronomy, Rice University, Houston, Texas, U.S.A.

(Received 17 July, 1987)

Abstract. Volcanic plumes on the Jovian satellite Io may be a visible manifestation of a plasma-arc discharge phenomenon. The amount of power in the plasma arc ($\sim 10^{11}$ W) is not enough to account for all the energy dissipated by the volcanoes. However, once a volcano is initiated by tidal and geologic processes, the dynamics of the volcanic plumes can be influenced by the plasma arcs. As initially pointed out by Gold (1979), plasma arcs are expected because of $\sim 10^6$ A currents and 400 kV potentials generated by the flow past Io of a torus of relatively dense magnetospheric plasma. We utilize our experience with laboratory plasma arcs to investigate the plume dynamics. The filamentation in the plume of the volcano Prometheus and its cross-sectional shape is quantitatively consistent with theories developed from laboratory observation.

1. Introduction

In the late 1950's and early 1960's, H. Alfvén directed a program of research on the physics of the plasma gun (Lindberg and Jacobsen, 1961, 1964; Dattner and Eninger, 1964; Wilcox *et al.*, 1964). As discussed by Wilcox *et al.*, one of the reasons motivating this research involved the origin of the planets and satellites (Alfvén, 1960; Alfvén and Wilcox, 1962). The apparent filamentary penumbra on Io may be the first direct verification of the plasma gun mechanism at work in the solar system.

The satellite Io was observed by the spacecraft Voyager 1 and Voyager 2 to be covered with volcanoes (Morabite *et al.*, 1979; Smith *et al.*, 1979; Strom *et al.*, 1979; Strom and Schneider, 1982). Nine active volcanoes were observed during the Voyager 1 encounter, eight of which were still active during the Voyager 2 flyby four months later. Detailed pictures of the plumes from one of these volcanoes were rather striking in that the plume material was ejected in a well-defined cone whose geometry showed converging (rather than diverging) matter at large lateral distances from the vent, and the plume material was concentrated into striations. Thus, we have a volcanic vent with exit velocities of about 0.5 km s^{-1}, but with the volcanic effluent concentrated into a cone with a half angle initially less than about 25° to the vent axis, and the material in the cone further

* Paper dedicated to Professor Hannes Alfvén on the occasion of his 80th birthday, 30 May 1988.

Astrophysics and Space Science **144** (1988) 451–461.

tending to concentrate into filaments that terminate on a narrow, well-defined, concentric annulus (Strom and Schneider, 1982).

We wish to raise the possibility that details of the volcanic discharge are a manifestation of a plasma arc at the volcanic vent as initially suggested by Gold (1979).

2. Plasma Gun Arc Discharge Mechanism

The plasma gun or plasma focus (Alfvén, 1958; Lindberg *et al.*, 1960; Lindberg and Jacobsen, 1961; Filippov *et al.*, 1962; Alfvén and Fälthammar, 1963; Mather, 1971; Bostick *et al.*, 1975; Alfvén *et al.*, 1981) is a plasma discharge consisting of a short but finite z-pinch which forms near or at the end of a coaxial plasma discharge. In the laboratory, the coaxial discharge is formed by switching a charged capacitor bank between a center electrode and an outer conducting tube electrode (Figure 1). The discharge is manifested by a current sheath, called a penumbra, that forms between the inner and outer electrodes when the inner electrode is at a positive potential (i.e., an anode) and the outer electrode is at ground (i.e., a cathode). The current sheath is equally well-defined whether the inner electrode is at a positive or negative potential but ion and neutron production at the focus are observed only when the inner electrode is an anode. Part of the stored magnetic energy in the tube and external circuit is rapidly converted to plasma energy during the current sheath's collapse toward axis. The current flow convergence is largely due to the self-consisting nature of the current filament, whereas

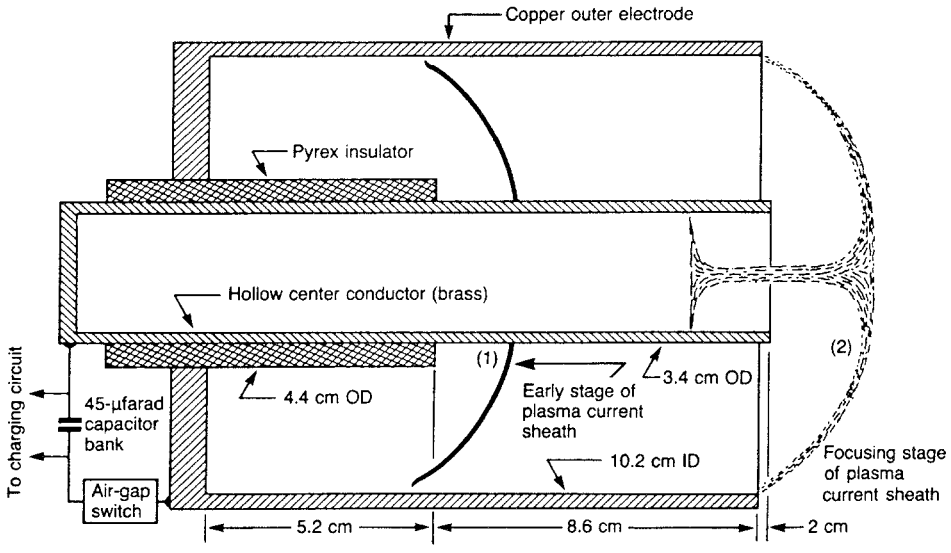

Fig. 1. Typical plasma gun apparatus. A capacitor bank is discharged through two coaxial electrodes forming a plasma current sheath between inner and outer electrodes. The $\mathbf{j} \times \mathbf{B}$ force accelerates the sheath outward to the ends of the electrodes where the inner sheath radius is forced inwards forming a columnar pinch or 'focus' on-axis. Also depicted on the diagram is the 'penumbra', the long-lived state of the current sheath at the muzzle of the plasma gun.

the heating and compression from the r, z implosion on the axis are due both to the magnetic forces of the current-carrying plasma filament and to inertial forces. Partial conversion of the kinetic energy of the imploding axisymmetric current to internal heat energy may occur during the implosive phase owing to self-collision.

Develoment of the plasma current leading to the formation of a plasma focus at the center electrode terminus can be conveniently subdivided into three main phases. First is the initial gas breakdown and the formation of a parabolic current front. Second is the hydromagnetic acceleration of a current sheath toward the open end. The third part

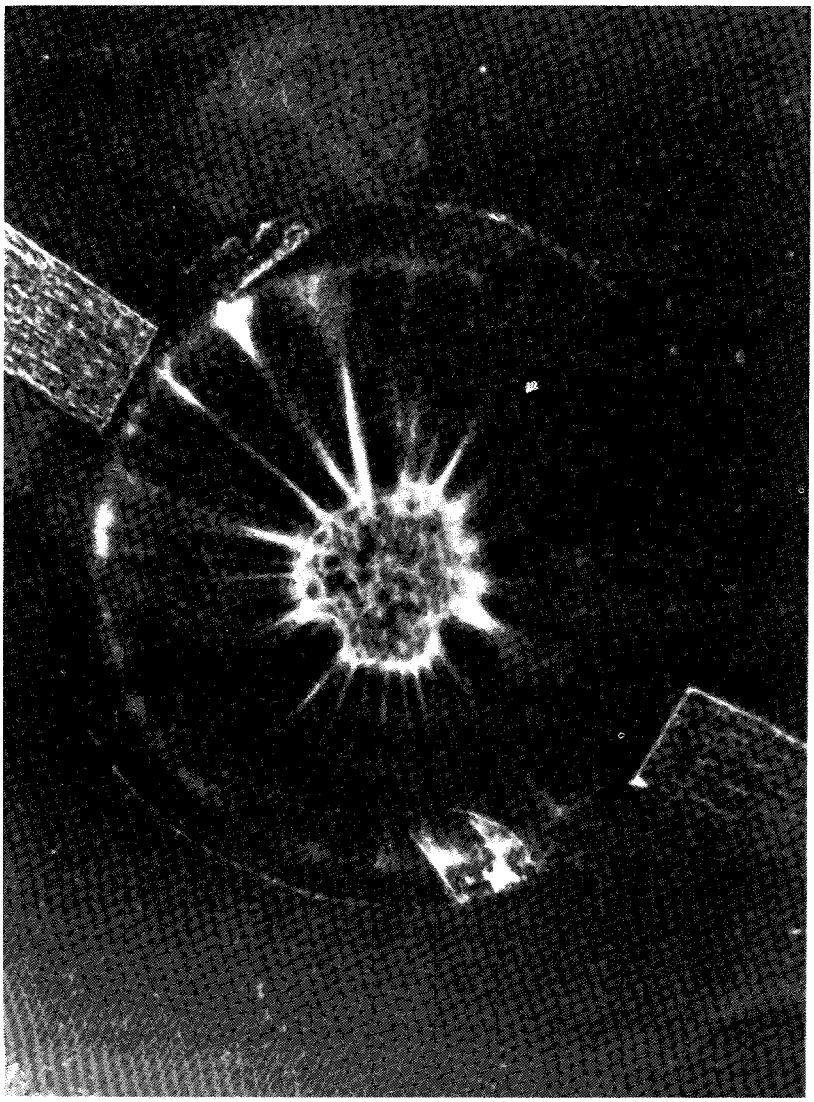

Fig. 2. End-on recording of the plasma gun penumbra.

of the discharge is the rapid collapse of the azimuthally-symmetric current sheath toward the axis to form the plasma focus.

2.1. BREAKDOWN PHASE

The breakdown has a radial, striated light pattern with a definite multifilamentary structure (Figure 2). This structure, except for its obvious radial striation, appears cylindrically symmetric (Figures 1 and 3). As the current increases, the terminus of this visible pattern moves radially outward until it reaches the outer electrode. The current front motion is best described as an unpinch or inverse process; i.e., the $(\mathbf{j} \times \mathbf{B})_r$ body force is exerted outward between the center electrode surface and the plasma current sheath. During this inverse phase, the sheath remains stable because of the stability of the inverse pinch process (the B_θ lines are convex).

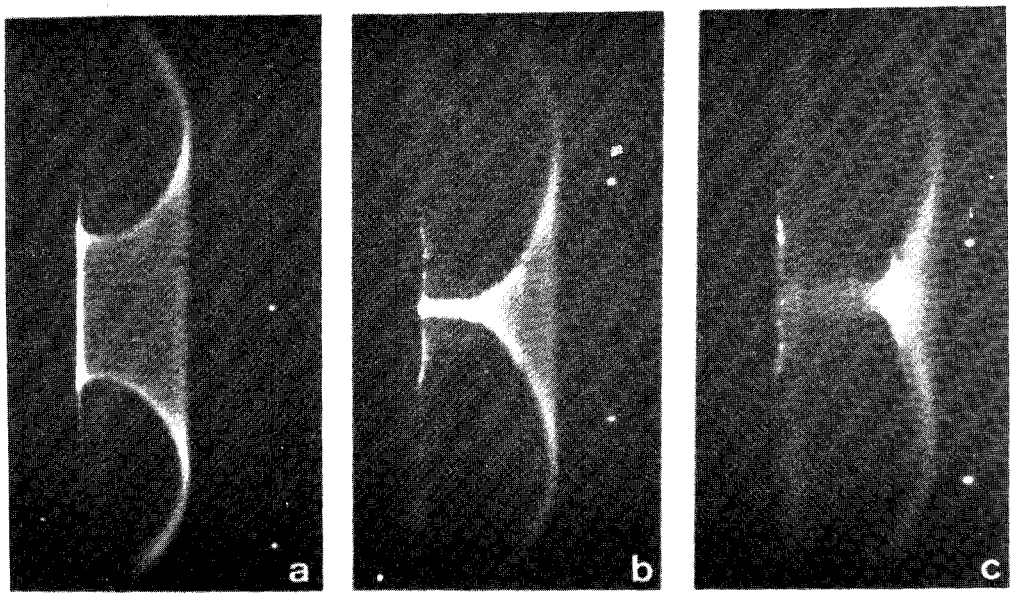

Fig. 3. Side-on image converter photographs of the plasma penumbra. (a) Before columnar collapse or pinch. (b) During pinch or focus.

The filamentary structures within the focus, rather than blending together, form a finite number of intense radial spokes ('spider legs'). These spokes appear to retain their identity throughout the acceleration phase and finally coalesce or focus on axis beyond the end of the center electrode, forming a thin circular annulus (Figure 2).

2.2. ACCELERATION PHASE

The current sheath across the annulus Δr is not planar, but canted backward from the anode to the cathode owing to the radial dependence of the magnetic pressure gradient. The total acceleration force $\mathbf{j} \times \mathbf{B}$ acting perpendicular to the current boundary leads to radial and axial motion. The $(\mathbf{j} \times \mathbf{B})_r$ radial component is outward and forces the current sheath to be annular at the outer electrode. The axial force $(\mathbf{j} \times \mathbf{B})_z$ varies as $1/r^2$ across the annulus and leads to higher sheath velocities near the surface of the center electrode. In the laboratory, fast image converter photographs distinctly show a parabolic current front. Owing to the parabolic current boundary, plasma flows centrifugally outward from anode to cathode along the current bounday as the acceleration continues. Plasma is seen to progress radially outward and beyond the outer electrode diameter as the current front accelerates downstream.

The overall time for plasma sheath acceleration to the end of the center electrode is related to the discharge potential across the annulus and the mass density of the background gas. For the case in which the current sheath pushes the gas ahead of the sheath, the sheath velocity is

$$v_s = \left[\frac{c^2 E^2}{4\pi\rho_0}\right]^{1/4}, \tag{1}$$

where E and ρ_0 are the discharge field strength and initial mass density, respectively (c.g.s. units).

2.3. COLLAPSE PHASE

The third phase encompasses the rapid convergence of the axisymmetric current sheath to the axis and the conversion of stored magnetic energy to plasma energy in the focus. The r, z convergence is due to the $\mathbf{j} \times \mathbf{B}$ pinch force. With this configuration, there is no equilibrium along the axis; hence, the plasma may readily escape axially in either direction. By the very nature of the convergence, much of the gas that the sheath encounters during collapse is ejected downstream and lost. The gas trapped in the focus is estimated as $\sim 10\%$ of that originally present.

The pinch effect is perhaps the most efficient way of heating and compressing a plasma. As the pinch induced implosion velocity of the current boundary imparts the same velocity to both ions and electrons, and because of the ion-electron mass difference, most of the energy appears as kinetic energy of the ions. In pinch devices, the ions are preferentially heated.

2.4. DYNAMIC BEHAVIOUR OF THE CURRENT SHEATH

The dynamic behaviour of the plasma current sheath can be analyzed using the measured time-dependent values of the voltage $V(t)$ across the electrodes, the tube current $I(t)$, and the sheath resistance $R(t)$.

The circuit equation representing the voltage across the electrodes *ab* in the equivalent

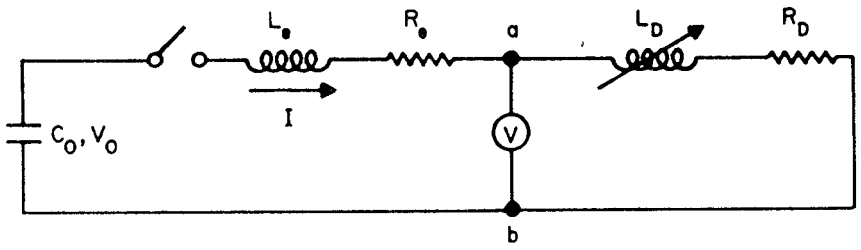

Fig. 4. Equivalent electrical circuit of the plasma gun discharge. The subscripts e and D denote external and discharge circuit elements, respectively.

electrical circuit (Figure 4) is

$$V(t) = (\mathrm{d}/\mathrm{d}t)\,[L_D(t)I(t)] + I(t)R_D(t)\,. \tag{2}$$

The part of the circuit to the left of ab in Figure 4 represents the electrical discharge and external circuit resistance R_e and external parasitic inductance L_e. The circuit to the left of ab represents the discharge inductance $L_D(t)$ and resistance $R_D(t)$.

By use of Equation (2), the following quantities are calculated.

(a) Discharge inductance:

$$L_D(t) = \int_0^{t'} [V(t) - I(t)R(t)]\,\mathrm{d}t/I(t)\,. \tag{3}$$

(b) Magnetic energy storage:

$$W_B(t) = \tfrac{1}{2}(L_e + L_D)I^2\,. \tag{4}$$

(c) Mechanical energy of the sheath:

$$W_s(t) = \frac{1}{2}\int_0^{t'} \dot{L}_D I^2\,\mathrm{d}t\,, \tag{5}$$

where $\mathrm{d}/\mathrm{d}t(L_D)$ is obtained from Equation (2).

(d) Pinch voltage during collapse:

$$V_p(t) = \dot{L}_D I + IR_D\,. \tag{6}$$

The instantaneous mass of the plasma sheath can be estimated using the momentum equation $\mathrm{d}(\rho\mathbf{v})/\mathrm{d}t = \mathbf{j} \times \mathbf{B}$,

$$m_0(t) = \left[10^{-7}\int_0^{t_c} I^2 \ln(r_o/r_i)\,\mathrm{d}t\right] v^{-1}\,, \tag{7}$$

where $v = v_s$ is the sheath velocity and r_o/r_i the ratio of the outer to inner electrode radii.

The upper integration limit t_c is the time to inner penumbra plasma collapse or pinch on axis.

3. The Plasma Gun Mechanism on Io

Plasma in Jupiter's magnetosphere injected from Io (the Io plasma torus) flows pas Io with a speed of about 57 km s^{-1}. The magnetic field from Jupiter at Io is 1900 nT. The $\mathbf{v} \times \mathbf{B}$ voltage induced across Io (3630 km) is, therefore, 400 kV, and approximately 10^6 A was observed to be flowing out of the satellite (Acuna *et al.*, 1981; Southwood *et al.*, 1980). It would seem plausible that the current would tend to concentrate in the volcanic plumes, which would give the current easy access to the highly conducting molten interior of Io. We would suppose that the crust, consisting of sulfer and frozen sulfer dioxide, would be a relatively poor conductor, thus directing the current to the volcanic vents. If we assume the available power (~ 0.4 TW) is equally divided between the four largest volcanic plumes, we have $\sim 10^{11}$ W of continuous power available for each volcanic plasma arc. This is roughly equal to the kinetic energy flux of material issuing from volcanic vent. A small fraction of this power can account for the faint auroral glow reported by Cook *et al.* (1981).

Figure 5 illustrates the basic geometry at hand. Viewed from the north Jovian and Ionian poles, Jupiter's dipole magnetic field is into the plane of the figure while the plasma flow within the torus is counter-clockwise toward Io. With this orientation, the

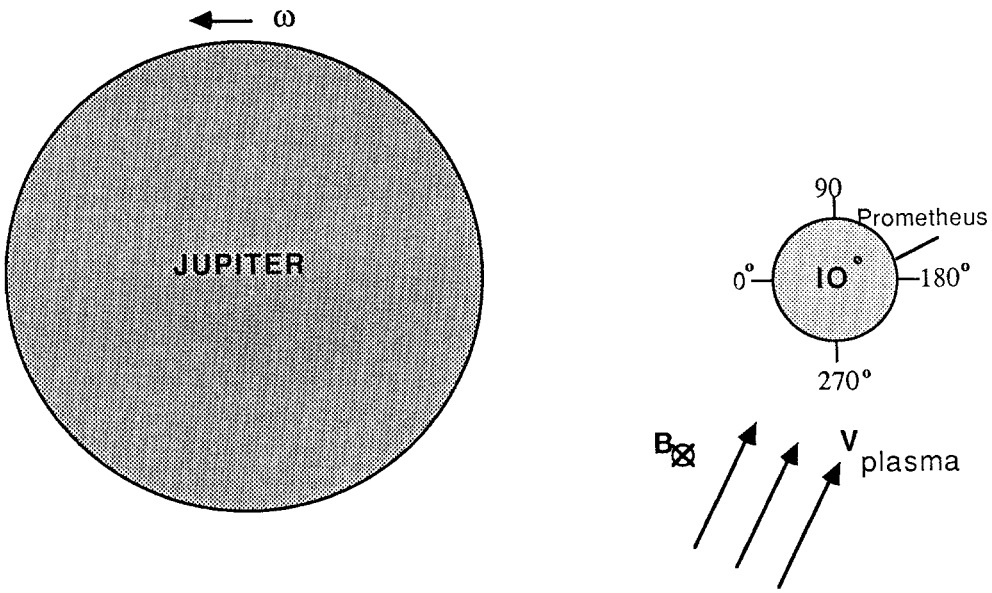

Fig. 5. The Jupiter-Io system (north pole view). The rotational period of Jupiter is approximately 9^h50^m. The orbital (synchronous) period of Io is 1.770 days. The relative velocity of the plasma torus flowing past Io is 57 km s^{-1}. (Diagram is not to scale.)

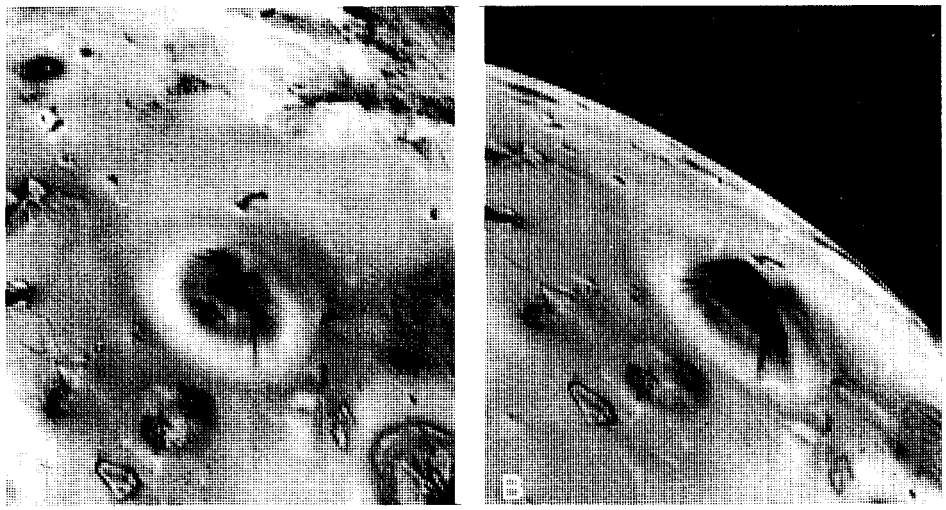

Fig. 6. Voyager 1 oblique views of Prometheus's plume. The left-hand image (A) was taken 2.3 hours before the right-hand image (B).

Fig. 7. Horizon view of Prometheus's plume.

electric field is directed from Jupiter to Io. Volcanic activity on Io generally occurs within an equatorial band of $\pm 30°$ latitude.

Figures 6 and 7 are photographs of the particularly well-developed volcanic plume Prometheus (latitude, $-2.9°$; longitude, 153°) taken at two different aspect angles by Voyager 1. The height and width of this plume is 77 km and 272 km, respectively (Strom and Schneider, 1982) while the vent velocity of the gaseous material ejected is 0.49 km s^{-1}. The current flow is outward from Prometheus, i.e., the vent of Prometheus is an anode. To relate these pictures to the plasma-arc process described in Section 2, we must explicitly assume that the fine particulate matter that makes the volcanic plumes visible is entrained by the plasma. Thus, as the plasma moves to form filaments, we assume that the plasma carries with it the small solid particles.

While an exact calculation of the breakdown field associated with a volcanic arc discharge requires precise knowledge about the region where the breakdown occurs*, an estimate can be made in the following way. For air, nitrogen, freon, and sulfur hexafluoride, for a sufficiently large separation between anode and cathode electrodes, the breakdown field can be expressed (Miller, 1982) in the form

$$E_{br}(\text{kV cm}^{-1}) = 24.6pF^{-1}, \tag{8}$$

where p is the pressure of the ambient gas in atmospheres and F represents a field enhancement factor of order unity that depends on the shapes of the anode and cathode. Applying Equation (8) to SO_2, the most common gas on Io, while setting $F = 1$ and taking an ambient pressure of the gas near the vapour-liquid transition (the triple point for SO_2 is 0.0163 atmospheres), yields $E_{br} = 0.4$ kV cm^{-1}. This value is to be compared to the breakdown field strength for lightning on Earth; 4.4 kV cm^{-1}.

Substituting $E = 0.4$ kV cm^{-1} and $\rho_0 = 2$ g cm^{-3} into Equation (1), we obtain a parabolic sheath velocity of $v_s = 0.893$ km s^{-1}. It is at this velocity that gas and plasma are pushed into Io's upper atmosphere by means of the arc discharge mechanism. The volcanoe effluent is concentrated into a penumbra whose morphology differs from those of ballastic or shock models in two ways. The first is the radial striations resulting from the electromagnetic pinch and accretion of matter into filaments (Figures 2 and 6). The second is the termination of the penumbra on a narrow cathode annulus (Figures 3 and 7).

4. Summary

Volcanic plumes on the Jovian satellite Io may be a visible manifestation of a plasma-arc discharge phenomenon. As pointed out by Gold (1979), plasma arcs are expected because of $\sim 10^6$ A currents and 400 kV potentials generated by the flow past Io of a torus of relatively dense ($2–3 \times 10^3$ cm^{-3}) magnetospheric plasma.

In this paper, the penumbra of current sheath produced in an arc discharge (Figures 2

* Comparison of the side-on penumbra morphology (Figures 1 and 3) to the side-on plume morphology (Figure 7) suggests that the location of the electrical discharge may be well below the surface of Io.

and 3) has been compared to photographs of the plume Prometheus (Figures 6 and 7). Both penumbra and plume are found to share a common morphology, i.e., a parabolic sheath profile, filamentation of matter within the sheath, and the termination of the sheath onto a rather thin annular ring. Moreover, the effluent ejection velocity as calculated from an expression for the sheath velocity in a plasma gun (0.893 km s^{-1}) is close to that observed for Prometheus, 0.49 km s^{-1}.

Motivated by a theory of the origin of the planets and satellites, H. Alfvén, in the late 1950's and early 1960's, directed a program of research on the physics of the plasma gun: the progenitor of the plasma focus discharge (Filippov, 1962; Mather, 1971). The apparent filamentary penumbra on Io may be the first direct verification of the plasma gun arc discharge mechanism at work in the solar system.

Acknowledgements

We thank Torrence Johnson for several encouraging and helpful comments. This work was supported by the U.S. Department of Energy and the National Aeronautics and Space Administration.

References

Acuna, M. H., Neubauer, F. M., and Ness, N. F.: 1981, *J. Geophys. Res.* **86**, 8513.

Alfvén, H.: 1958, in *Proceedings of the 2nd Int. Conf. on Peaceful Uses of Atomic Energy*, United Nations, Geneva, Vol. 31, p. 3.

Alfvén, H.: 1960, *On the Origin of the Solar System*, Oxford University Press, New York (see also *Rev. Mod. Phys.* **32**, 710).

Alfvén, H.: 1981, *Cosmic Plasma*, D. Reidel Publ. Co., Dordrecht, Holland, Ch. IV.

Alfvén, H. and Fälthammar, C.-G.: 1963, *Cosmic Electrodynamics*, Oxford University Press, London.

Alfvén, H. and Wilcox, J. M.: 1962, *Astrophys. J.* **136**, 1016.

Bostick, W. H., Nardi, V., and Prior, W.: 1975, *Ann. N.Y. Acad. Sci.* **251**, 2.

Cook, A. F., Shoemaker, E. M., Smith, B. A., Danielson, G. E., Johnson, T. V., and Synnott, S. P.: 1981, *Science* **211**, 1419.

Dattner, A. and Eninger, J.: 1964, *Phys. Fluids Suppl.* **7**, S41.

Filippov, N. V., Filippova, T. I., and Vinogradov, V. P.: 1962, *Nucl. Fusion Suppl.*, Pt. 2.

Fowler, T. K. and Coengens, F. H.: 1979, *9th Eur. Conf. Controlled Fusion and Plasma Physics*, Oxford, September 1979.

3rd Symp. on Physics and Technology of Compact Toroids in the Magnetic Fusion Energy Program, Los Alamos, 1980, Los Alamos National Laboratory Report LA-8700-C (1981).

Gerdin, G., Stygar, W., and Venneri, F.: 1981, *J. Appl. Phys.* **52**, 3269.

Gold, T.: 1979, *Science* **206**, 1071.

Goldenbaum, G. C., Irby, I. H., Chong, Y. P., and Hart, G.: 1979, *9th Eur. Conf. Controlled Fusion and Plasma Physics*, Oxford, September 1979.

Koloc, P. and Ogden, J.: 1979, *Symp. on Compact Toruses and Energetic Particle Injection*, Princeton Univ., December 1979.

Latham, R. V.: 1982, *Xth Int. Symp. on Discharge and Electrical Insulation in Vacuum*, Columbia, South Carolani, IEEE Cat. No. 82CH1826-7, p. 3.

Lindberg, L. and Jacobsen, C. T.: 1961, *Astrophys. J.* **133**, 1043.

Lindberg, L. and Jacobsen, C. T.: 1964, *Phys. Fluids Suppl.* **7**, S44.

Lindberg, L., Witalis, E., and Jacobsen, C. T.: 1960, *Nature* **185**, 452.

Mather, J. W.: 1971, in R. H. Lovberg and H. R. Griem (eds.), *Plasma Physics*, Academic Press, New York, Ch. 15.

Miller, R. B.: 1982, *Intense Charged Particle Beams*, Plenum, New York, Ch. 1.
Morabite, L. A., Synnott, S. P., Kupferman, P. N., and Collins, S. A.: 1979, *Science* **204**, 972.
Ness, N. F. *et al.*: 1979, *Science* **204**, 982.
Smith, B. A. *et al.*: 1979, *Science* **204**, 945.
Smith, B. A., Shoemaker, E. M., Kieffer, S. W., and Cook, A. F.: 1979, *Nature* **280**, 738.
Southwood, D. J., Kivelson, M. G., Walker, R. J., and Slavin, J. A.: 1980, *J. Geophys. Res.* **85**, 5959.
Strom, R. G. and Schneider, N. M.: 1982, in D. Morrison (ed.), *Satellites of Jupiter*, Univ. Arizona Press, Tucson, Arizona, p. 598.
Strom, R. G., Terrile, R. J., Masursky, H., and Hansen, C.: 1979, *Nature* **280**, 733.
Wilcox, J. M., Pugh, E., Dattner, A., and Eninger, J.: 1964, *Phys. Fluids Suppl.* **7**, S51.